Free Radical Biology & Medicine 52 (2012) 1828–1834

Contents lists available at SciVerse ScienceDirect

Free Radical Biology & Medicine

journal homepage: www.elsevier.com/locate/freeradbiomed

Original Contribution

A new SOD mimic, Mn(III) *ortho N*-butoxyethylpyridylporphyrin, combines superb potency and lipophilicity with low toxicity

Zrinka Rajic [a,1], Artak Tovmasyan [a], Ivan Spasojevic [b], Huaxin Sheng [c], Miaomiao Lu [c,d], Alice M. Li [e,2], Edith B. Gralla [e], David S. Warner [c], Ludmil Benov [f], Ines Batinic-Haberle [a,*]

[a] *Department of Radiation Oncology, Duke University Medical Center, NC 27710, USA*
[b] *Department of Medicine , Duke University Medical Center, NC 27710, USA*
[c] *Department of Anesthesiology, Duke University Medical Center, NC 27710, USA*
[d] *Department of Anesthesiology, Second Affiliated Hospital, Zhengzhou University, Henan, China*
[e] *Department of Chemistry and Biochemistry, UCLA, Los Angeles, CA 90095-1569, USA*
[f] *Department of Biochemistry, Faculty of Medicine, Kuwait University, 13110 Safat, Kuwait*

ARTICLE INFO

Article history:
Received 3 November 2011
Revised 17 January 2012
Accepted 3 February 2012
Available online 13 February 2012

Keywords:
SOD mimic
MnTnHex-2-PyP^{5+}
MnTnBuOE-2-PyP^{5+}
Drug toxicity

ABSTRACT

The Mn porphyrins of $k_{cat}(O_2^{\bullet-})$ as high as that of a superoxide dismutase enzyme and of optimized lipophilicity have already been synthesized. Their exceptional *in vivo* potency is at least in part due to their ability to mimic the site and location of mitochondrial superoxide dismutase, MnSOD. MnTnHex-2-PyP^{5+} is the most studied among lipophilic Mn porphyrins. It is of remarkable efficacy in animal models of oxidative stress injuries and particularly in central nervous system diseases. However, when used at high single and multiple doses it becomes toxic. The toxicity of MnTnHex-2-PyP^{5+} has been in part attributed to its micellar properties, i.e., the presence of polar cationic nitrogens and hydrophobic alkyl chains. The replacement of a CH_2 group by an oxygen atom in each of the four alkyl chains was meant to disrupt the porphyrin micellar character. When such modification occurs at the end of long alkyl chains, the oxygens become heavily solvated, which leads to a significant drop in the lipophilicity of porphyrin. However, when the oxygen atoms are buried deeper within the long heptyl chains, their excessive solvation is precluded and the lipophilicity preserved. The presence of oxygens and the high lipophilicity bestow the exceptional chemical and physical properties to Mn(III) *meso*-tetrakis(*N*-*n*-butoxyethylpyridinium-2-yl)porphyrin, MnTnBuOE-2-PyP^{5+}. The high SOD-like activity is preserved and even enhanced: log $k_{cat}(O_2^{\bullet-}) = 7.83$ vs 7.48 and 7.65 for MnTnHex-2-PyP^{5+} and MnTnHep-2-PyP^{5+}, respectively. MnTnBuOE-2-PyP^{5+} was tested in an $O_2^{\bullet-}$ -specific *in vivo* assay, aerobic growth of SOD-deficient yeast, *Saccharomyces cerevisiae*, where it was fully protective in the range of 5–30 μM. MnTnHep-2-PyP^{5+} was already toxic at 5 μM, and MnTnHex-2-PyP^{5+} became toxic at 30 μM. In a mouse toxicity study, MnTnBuOE-2-PyP^{5+} was several-fold less toxic than either MnTnHex-2-PyP^{5+} or MnTnHep-2-PyP^{5+}.

Abbreviations: $O_2^{\bullet-}$, superoxide; SOD, superoxide dismutase; H_2TnBuOE-2-PyP^{4+}, *meso*-tetrakis(*N*-n-butoxyethylpyridinium-2-yl)porphyrin; MnPs, Mn(III) *N*-alkyl- and *N*-alkoxyalkylpyridylporphyrins; Mn^{II}P and Mn^{III}P, Mn porphyrins with Mn in its +2 and +3 oxidation states; MnTE-2-PyP^{5+} (AEOL10113, FBC007), Mn(III) *meso*-tetrakis(*N*-ethylpyridinium-2-yl)porphyrin; MnTnBu-2-PyP^{5+}, Mn(III) *meso*-tetrakis(*N*-*n*-butylpyridinium-2-yl)porphyrin; MnTMOE-2-PyP^{5+}, Mn(III) *meso*-tetrakis(*N*-methoxyethylpyridinium-2-yl)porphyrin; MnTnHex-2-PyP^{5+}, Mn(III) *meso*-tetrakis(*N*-*n*-hexylpyridinium-2-yl)porphyrin; MnTnHep-2-PyP^{5+}, Mn(III) *meso*-tetrakis(*N*-*n*-heptylpyridinium-2-yl)porphyrin; MnTnOct-2-PyP^{5+}, Mn(III) *meso*-tetrakis(*N*-*n*-octylpyridinium-2-yl)porphyrin; MnTMOHex-2-PyP^{5+}, Mn(III) *meso*-tetrakis(*N*-(6′-methoxyhexyl)pyridinium-2-yl)porphyrin; MnTMOHex-3-PyP^{5+}, Mn(III) *meso*-tetrakis(*N*-(6′-methoxyhexyl)pyridinium-3-yl)porphyrin; MnTnBuOE-2-PyP^{5+} (BMX-001), Mn(III) *meso*-tetrakis(*N*-*n*-butoxyethylpyridinium-2-yl)porphyrin; MnTnBuOE-3-PyP^{5+}, Mn(III) *meso*-tetrakis(*N*-*n*-butoxyethylpyridinium-3-yl)porphyrin; R_f, thin-layer chromatographic retention factor that presents the ratio between the compound and the solvent path in 1:1:8 = $KNO_{3(sat)}$:H_2O:CH_3CN solvent system; $E_{1/2}$, half-wave reduction potential; NHE, normal hydrogen electrode; P_{OW}, partition between *n*-octanol and water; ip, intraperitoneal; $k_{cat}(O_2^{\bullet-})$, the rate constant for the catalysis of $O_2^{\bullet-}$dismutation; HFBA, heptafluorobutyric acid.

* Corresponding author at: Department of Radiation Oncology–Cancer Biology, Duke University Medical Center, Research Drive, 281b/285 MSRB I, Box 3455, Durham, NC 27710. Fax: +1 919 684 8718.
E-mail address: ibatinic@duke.edu (I. Batinic-Haberle).
[1] Present address: Department of Medicinal Chemistry, Faculty of Pharmacy and Biochemistry, University of Zagreb, A. Kovacica 1, Zagreb, Croatia.
[2] Present address: Yale School of Medicine, New Haven, CT 06510, USA.

0891-5849/$ – see front matter © 2012 Elsevier Inc. All rights reserved.
doi:10.1016/j.freeradbiomed.2012.02.006

Introduction

Mn porphyrin-based SOD mimics, peroxynitrite scavengers, and redox modulators of cellular signaling pathways have been developed for over 20 years [1–5]. The optimization of their structure took place in three phases. In Phase I, we aimed at achieving the potency of SOD enzymes, i.e., the rate constant for the catalysis of $O_2^{\cdot-}$ dismutation as close as possible to log $k_{cat}(O_2^{\cdot-}) = 8.84–9.30$. Over the years we have explored a number of porphyrins and established the structure–activity relationships (SAR) for cationic, neutral, and anionic Mn porphyrins [1–3]. The SAR relates the SOD-like potency (expressed in terms of k_{cat}) to the thermodynamic parameter, reduction potential for the $Mn^{III}P/Mn^{II}P$ redox couple, $E_{1/2}$. In Fig. 1 the SAR is shown for cationic MnPs only. The presence of charges on an SOD mimic close to the Mn site in *ortho* positions of pyridyl rings affords both thermodynamic and kinetic facilitation for the $O_2^{\cdot-}$ dismutation [1–3,5].

Based on SAR and our simple $O_2^{\cdot-}$-specific *in vivo* model of the aerobic growth of SOD-deficient *E. coli*, the *ortho* isomeric Mn(III) *N*-substituted pyridylporphyrins have emerged as the most potent and stable SOD mimics with log k_{cat} ~8. Among them, MnTE-2-PyP^{5+} has been the most frequently studied compound.

As research progressed it became obvious that *in vivo* efficacy depends on the bioavailability of the compound also, i.e., its tissue, cellular, and subcellular distribution, which in turn depends on its lipophilicity, charge, size, shape, and bulkiness. In Phase II, while maintaining the total charge and its position, we lengthened the alkyl chains from methyl to octyl. Such modification largely increased the efficacy of MnPs in ameliorating central nervous system injuries, such as stroke, subarachnoid hemorrhage, pain, and cerebral palsy [1,6,7]. Among the lipophilic analogs, MnTnHex-2-PyP^{5+} has been the most frequently studied porphyrin [1,3,6]. The remarkable efficacy of MnTE-2-PyP^{5+} and MnTnHex-2-PyP^{5+} in numerous animal models of oxidative stress diseases [1,3,8–10] may be at least in part attributed to their ability to accumulate in mitochondria, mimicking therefore the site and the action of critical mitochondrial enzyme, MnSOD [7]. Mitochondrial accumulation of lipophilic MnTnHex-2-PyP^{5+} was significantly enhanced when compared to a more hydrophilic MnTE-2-PyP^{5+} [7].

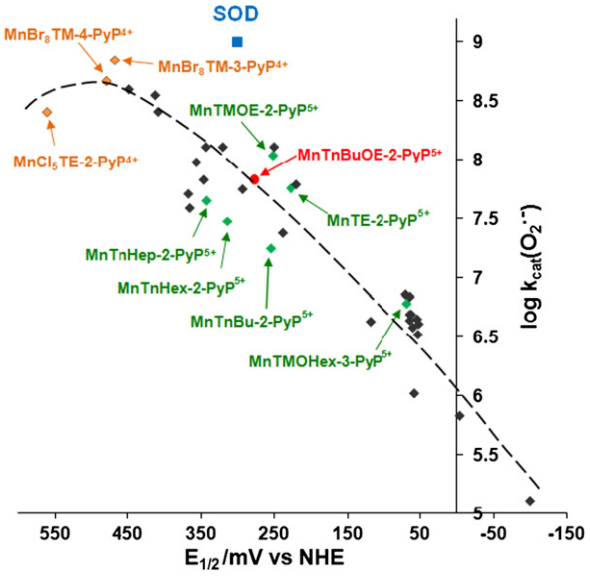

Fig. 1. Structure–activity relationship between the redox property of cationic Mn porphyrins, $E_{1/2}$ (reduction potential for the $Mn^{III}P/Mn^{II}P$ redox couple), and the SOD-like potency, log $k_{cat}(O_2^{\cdot-})$. The data for the SOD enzyme are also shown. The optimized SOD mimics with regard to metal/ligand stability and log k_{cat} are *ortho* Mn(III) *N*-substituted pyridylporphyrins with $E_{1/2}$ in between +200 and +400 mV vs NHE.

In an ongoing Phase III we aimed at suppressing the toxicity of lipophilic *N*-alkylpyridylporphyrins. The toxicity of MnTnHex-2-PyP^{5+} at higher concentrations/doses is at least in part due to its micellar property, and thus ability to damage membranes [11,12]. We already observed that the replacement of a CH_2 group by oxygen atom in each of the four butyl chains suppressed the toxicity of MnTnBu-2-PyP^{5+}, but unfortunately, it greatly decreased its lipophilicity also [4]. We applied the same approach to the modification of a lipophilic MnTnHex-2-PyP^{5+}, attaching methoxy groups at the end of the hexyl chains, hoping that in this case the lipophilicity of the longer hexyl chains would outbalance the polarity of oxygens. Yet, the methoxyhexyl derivative MnTMOHex-2-PyP^{5+} is significantly less lipophilic in comparison with its parent MnTnHex-2-PyP^{5+} [13]. In this work, we showed that if the oxygen atoms are buried within the long-alkyl chains (closer to the pyridyl rings) of MnTnBuOE-2-PyP^{5+}, and are thus protected from the extensive solvation, the high lipophilicity is fully preserved. The toxicity of MnTnBuOE-2-PyP^{5+} to both mice and *Saccharomyces cerevisiae* is greatly decreased relative to either MnTnHex-2-PyP^{5+} (bearing the same number of carbon atoms in pyridyl substituents) or MnTnHep-2-PyP^{5+} (of the same length of pyridyl substituents).

Experimental

General

H_2T-2-PyP was purchased from Frontier Scientific. 2-Butoxyethanol (>99%) was from TCI America, *p*-toluenesulfonyl chloride (98%) from Alpha Aesar, and *tetra-n*-butylammonium chloride hydrate (98%) was from Aldrich. $MnCl_2 \times 4H_2O$ (99.7%) was supplied by J. T. Baker, and NH_4PF_6 (99.99% purity) was from GFS chemicals. Diethyl ether anhydrous and acetone were from EMD chemicals, while dichloromethane, chloroform, acetonitrile, EDTA, and KNO_3 were purchased from Mallinckrodt. *N,N*-Dimethylformamide anhydrous (99.8% purity), pyridine anhydrous (99.8%), and plastic-backed silica gel TLC plates were from Sigma-Aldrich. Xanthine and equine ferricytochrome *c* (Lot 7752) were from Sigma, whereas xanthine oxidase was prepared by R. Wiley [5]. Sodium sulfate anhydrous (>99%) was from Sigma-Aldrich. All chemicals were used as received without further purification. The porphyrins (MnTE-2-PyP^{5+}, MnTnHex-2-PyP^{5+}, and MnTnHep-2-PyP^{5+}) used throughout this study were synthesized according to the procedures described earlier [2].

Elemental analyses

Elemental analyses of the porphyrin ligand and its Mn complex were performed by Atlantic MicroLab (Norcross, GA, USA). All analyses were done in duplicates.

UV/vis spectra

UV/vis spectra were recorded in H_2O at room temperature on a UV-2501PC Shimadzu spectrophotometer with 0.5-nm resolution.

Electrospray ionization mass spectrometric (ESI-MS) analyses

The analyses were performed as described elsewhere [14] on an Applied Biosystems MDS Sciex 3200 Q Trap LC/MS/MS spectrometer at Duke Comprehensive Cancer Center, Shared Resource PK Labs. All samples of 1 μM concentrations were prepared in acetonitrile:H_2O (1:1, v/v; containing 0.01% v/v HFBA) mixture and infused for 1 min at 10 μl/min into the spectrometer (curtain gas 20 V, ion spray voltage 3500 V, ion source 30 V, $t = 300$ °C, declustering potential 20 V, entrance potential 1 V, collision energy 5 V, gas N_2) [15]. In the presence of soft anion, heptafluorobutyrate, which pairs with cationic

porphyrin, no fragmentation of the porphyrin has been detected. Thus any partially quaternized porphyrin found in the mass spectrum is the consequence of partial alkylation or alkoxyalkylation, but not of fragmentation during spectral analysis [14].

Synthesis

2-Butoxyethyl *p*-toluenesulfonate was prepared as already described [16]; spectroscopic data were in agreement with the proposed structure.

H_2TnBuOE-2-PyPCl$_4$

N-Butoxyethylation was performed as previously described for analogous alkyl derivatives [17]. To a solution of H_2T-2-PyP (40 mg, 0.0065 mmol) in anhydrous DMF (6.6 mL, preheated at 105 °C for 10 min) 2-butoxyethyl *p*-toluenesulfonate (8.8 g, 0.032 mol) was added. The course of the reaction was followed by TLC using 1:1:8 = $KNO_{3(sat)}$:H_2O:CH_3CN as a mobile phase. While atropisomers with lipophilic analogs of the *ortho* alkyl series separate on the TLC plate, under the same conditions with H_2TnBuOE-2-PyP^{4+} and its Mn complex they do not. Quaternization of sterically hindered *ortho* isomer was completed in ~3.5 days, observed as a single spot on a TLC plate. The reaction mixture was filtered into the separatory funnel containing H_2O and chloroform and extracted multiple times with chloroform. After filtration of the combined H_2O layers, the isolation of H_2TnBuOE-2-PyP^{4+} as a chloride salt was performed as previously described [17]. Elemental analysis: H_2TnBuOE-2-PyPCl$_4$ × 11.5 H_2O. Anal Calcd for $C_{64}H_{101}N_8O_{15.5}Cl_4$: C, 56.01; H, 7.42; N, 8.17; Cl, 10.33%. Found: C, 56.22; H, 7.02; N, 8.34; Cl, 10.21%.

MnTnBuOE-2-PyPCl$_5$

Metallation was achieved as previously described for alkyl analogs [17], with slight modifications. The aqueous solution of H_2TnBuOE-2-PyPCl$_4$ was basified with 0.1 M NaOH to pH ~10.7, which ensured a significant amount of reactive (OH)MnP species and deprotonation of inner pyrrolic nitrogens, both essential for successful metallation at room temperature. Metallation was performed with 20-fold excess of $MnCl_2 \times 4H_2O$ on whose addition the pH of the solution dropped to ~7.8 due to the extensive hydrolysis of Mn aqua ion. The course of metallation was monitored by TLC using 1:1:8 = $KNO_{3(sat)}$:H_2O:CH_3CN as a mobile phase, as well as by UV/vis spectroscopy. A very useful means to follow the completion of the metallation is to follow the loss of the ligand fluorescence under UV light (~350 nm). Completion of the metallation was achieved within hours at room temperature. MnP solution was filtrated (to remove Mn oxo/hydroxo species and MnO_2). The isolation of MnTnBuOE-2-PyP^{5+} as a chloride salt was performed as previously described [17]. Elemental analysis: MnTnBuOE-2-PyPCl$_5$ × 12.5 H_2O. Anal Calcd for $MnC_{64}H_{101}N_8O_{16.5}Cl_5$: C, 51.98; H, 6.88; N, 7.58; Cl, 11.99%. Found: C, 52.07; H, 6.71; N, 7.83; Cl, 11.76%.

Electrochemistry

Cyclic voltammetry was performed on a CH Instruments Model 600 voltammetric analyzer with MnTE-2-PyP^{5+} as a standard as previously described in detail [4,18].

Catalysis of $O_2^{\cdot-}$ dismutation (cytochrome *c* assay)

The ability of MnTnBuOE-2-PyP^{5+} to dismute $O_2^{\cdot-}$ was evaluated via cytochrome *c* assay which was proven to be equally effective as pulse radiolysis and stopped-flow methodology [2,3,19–22]. The experiments were conducted at room temperature (25 ± 1 °C) in 0.05 M potassium phosphate buffer, pH 7.8, 0.1 mM EDTA as reported elsewhere [19].

Stability of MnTnBuOE-2-PyP^{5+} toward HCl

We aimed to see if the compound would survive the stomach acidity when given per os. MnTnBuOE-2-PyP^{5+} was tested at pH 1, at 4, 24, and 48 h after acidification of ~0.5 mM and 5 μM solutions with hydrochloric acid. Due to the high levels of chloride, molecular ions bearing mixed chloride/heptafluorobutyrate counteranions were found in the mass spectrum. No changes were observed in UV/vis and ESI-MS spectra of MnP after acidification, indicating that neither loss of Mn nor the hydrolysis of ether bond happened.

Lipophilicity

Lipophilicity was determined as retention factor on TLC plates, R_f and as log P_{OW} as described earlier [15].

S. cerevisiae study

The wild-type *S. cerevisiae* strain used was EG103, which has a complete genotype of *MATα, leu2, his3, trp1, ura3*. The *sod1Δ* mutant *S. cerevisiae* strain, lacking Cu,ZnSOD, was EG118, which has a complete genotype of *MATα, leu2, his3, trp1, ura3*, *sod1Δ::URA3*. These strains, described by Gralla and Valentine [23], were first streaked from 20% glycerol stocks onto yeast extract, peptone agar supplemented with 2% dextrose (YPD) and incubated for 72 h at 30 °C under hypoxic conditions [24]. Single colonies were then selected to grow to stationary phase under hypoxic conditions at 30 °C in the above-noted medium supplemented with penicillin and streptomycin to prevent bacterial growth. The overnight cultures were diluted ~1000-fold with YPD medium. Absorbance at 600 nm (A_{600}) was checked and adjusted to be equal for both parental and *sod1Δ* mutant stock suspensions, and 200 μL aliquots were transferred into 96-well plates. Aqueous solutions of Mn porphyrins were filter-sterilized (0.22-μm filter, Whatman, Middlesex, UK). Cultures in 96-well plates were grown aerobically at 30 °C and 200 rpm on a thermostatic shaker. All samples were run in triplicates and in controls the volume was compensated with sterile distilled water. Growth was followed turbidimetrically by measuring the absorbance at 600 nm using an ELISA reader.

Mouse toxicity study

Eight- to 10-week-old male C57BL/6 J mice were used for the toxicity study. Body weight and rotarod performance were measured daily before and after MnP injections as described earlier [25,26]. Also, behavior and survival were closely observed immediately after the treatment with MnPs. All animal procedures conformed to the Institutional Animal Care and Use Committee and National Institute of Health guidelines. Mice were given intraperitoneal (ip) injections of saline, 0.5, 1.5, 4.5, or 9 mg/kg/day of MnTnBuOE-2-PyP^{5+} for 7 days (the total daily doses were given in two increments). Mice were placed on a rotarod with an accelerated speed of 4–40 rpm and latency to fall from the rotarod was automatically recorded. Data are expressed as percentage of the pretreatment baseline. Four mice were used per dose. In order to more accurately compare the toxicity among MnTnBuOE-2-PyP^{5+}, MnTnHex-2-PyP^{5+}, and MnTnHep-2-PyP^{5+}, an additional four mice per dose were also injected with single injection of 2.5 or 5 mg/kg MnTnHex-2-PyP^{5+}, 5 or 10 mg/kg MnTnBuOE-2-PyP^{5+}, and 2.5, 5 or 10 mg/kg MnTnHep-2-PyP^{5+}.

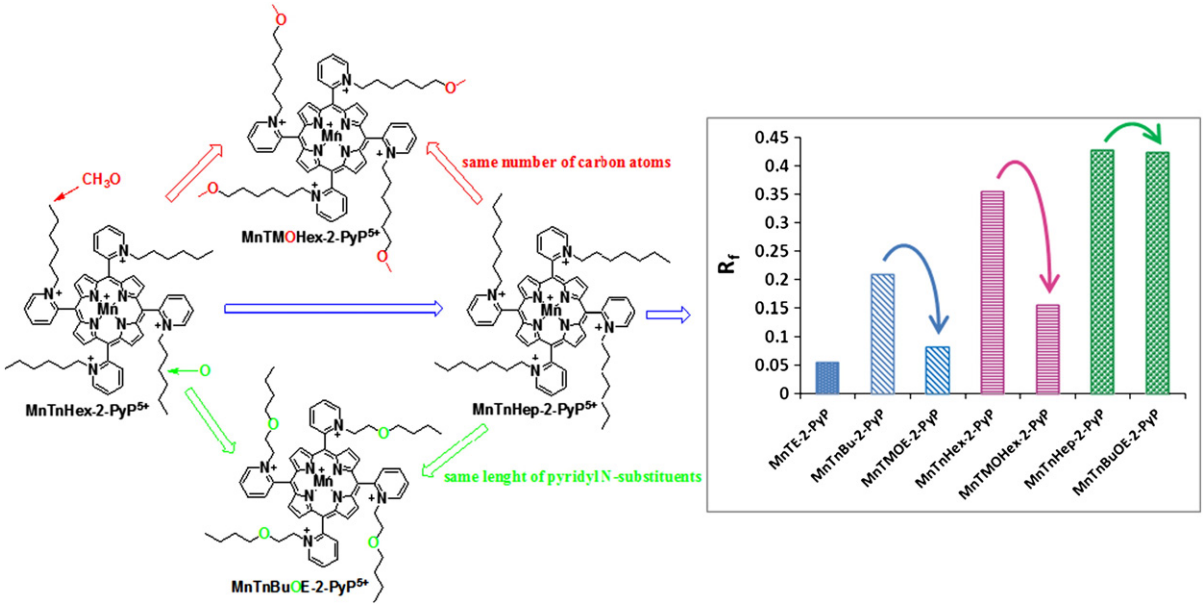

Fig. 2. The lipophilicity of Mn(III) *N*-alkyl- and *N*-alkoxyalkylpyridylporphyrins as determined by TLC chromatographic retention factor, R_f. The presence of the oxygen atoms at the periphery of the alkyl chains in MnTMOHex-2-PyP^{5+} results in their solvation and in turn causes a large drop in the lipophilicity relative to MnTnHex(nHep)-2-PyP^{5+}. However, when the pyridyl substituents in MnTnBuOE-2-PyP^{5+} are equally long but contain oxygens closer to the porphyrin ring, the solvation is minimized and therefore the lipophilicity is not significantly affected relative to MnTnHex(nHep)-2-PyP^{5+}.

Results and discussion

While of remarkable efficacy with single or multiple doses as low as 0.05 mg/kg [1–3], a lipophilic cationic MnTnHex-2-PyP^{5+} exerts toxicity at higher doses which is in part due to its micellar character. We hoped that the placement of oxygen atoms at the very end of the alkyl chains would not significantly diminish the porphyrin lipophilicity, but would disrupt the micellar character of the alkyl chains. Yet, this happened not to be the case: a significant drop in the lipophilicity of MnTMOHex-2-PyP^{5+} (as measured via chromatographic retention factor, R_f) relative to MnTnHex-2-PyP^{5+} was observed (Fig. 2). Moreover, during *N*-methoxyhexylation, the methoxyhexyl *p*-toluenesulfonate underwent intramolecular cyclization, which diminished the purity of the compound. Rather than interacting with pyridyl nitrogens only, the methoxyhexyl carbocation undergoes intramolecular cyclization with its own oxygen atom leading to the formation of a 7-membered ring. Subsequently, the oxygen–carbon bond of the methyl group weakens; in turn the methyl group leaves and methylates the pyridyl nitrogen. Due to the length of the quaternization process (~3.5 days), a significant amount of the species with three methoxyhexyl and one methyl groups was found in the preparation. The mechanistic aspects of the intramolecular cyclization leading to the unwanted product will be detailed in a subsequent publication [Rajic et al., in preparation, 27].

The quaternization of a *meta* isomer to form H$_2$TMOHex-3-PyP^{4+} was much faster (within hours). Subsequent metallation gave rise to MnTMOHex-3-PyP^{5+}; the preparation contains up to 5% of the species bearing one methyl group. To understand the origin of much higher amount of the porphyrin with three methoxyhexyl groups and one methyl group, we synthesized a number of porphyrins with different chain lengths and different positions of the oxygen atoms in the alkyl chains [Rajic et al., in preparation, 27]. The different position of the oxygens in alkoxyalkyl *p*-toluenesulfonate leads to the formation of cycles of different size and therefore different stability via intramolecular rearrangement; consequently more or less of the porphyrin species bearing one undesirable alkyl chain will be formed [27]. Such strategy led us to eventually explore the 2-butoxyethyl *p*-toluenesulfonate, and we ended up with a beautiful molecule of superior properties: MnTnBuOE-2-PyP^{5+}. With 2-butoxyethyl *p*-toluenesulfonate, the intramolecular cyclization within the $^{+}CH_2$–CH_2–O–CH_2–CH_2–CH_2–CH_3 group would be unfavorable due to the formation of an unstable 3-membered ring. Consequently, a insignificant amount of the porphyrin bearing three butoxyethyl groups and one butyl group could be expected. Indeed, that was the case. Moreover, we were pleasantly surprised that *the position of oxygen atoms buried deeper into the alkyl chains partly suppressed their solvation.*

Table 1
UV/vis absorption maxima, λ_{max} (nm) and molar absorption coefficients (ε, M^{-1} cm^{-1}) of H$_2$TnBuOE-2-PyPCl$_4$ and its Mn(III) complex.

(Metallo)porphyrin	λ_{max} nm (log ε)[a]
H$_2$TnBuOE-2-PyPCl$_4$	264.0 (4.35), 418.0 (5.36), 513.0 (4.25), 545.0 (3.61), 585.0 (3.84), 638.0 (3.38)
MnTnBuOE-2-PyPCl$_5$	213.5 (4.75), 262.5 (4.60), 365.0 (4.75), 412.0 (4.42), 455.5 (5.25), 559.5 (4.17), 783.0 (3.33)

[a] Spectra were taken in water at room temperature. Molar absorption coefficients (M^{-1} cm^{-1}) were determined within 5% errors. λ_{max} (nm) were determined with errors inside ± 0.5 nm.

Table 2
Electrospray ionization mass spectrometry (ESI-MS) data for H$_2$TnBuOE-2-PyP^{4+} (H$_2$P^{4+}) and its Mn(III) complex (MnP^{5+}).

Species	*m/z*	
	Found	Calcd
H$_2$P^{4+}/4	256.1	255.7
(H$_2$P^{4+}– H$^+$)$^{3+}$/3	340.9	340.5
(H$_2$P^{4+} + HFBA$^-$)$^{3+}$/3	412.2	411.9
(H$_2$P^{4+} + HFBA$^-$ – H$^+$)$^{2+}$/2	617.7	617.3
(H$_2$P^{4+} + 2HFBA$^-$)$^{2+}$/2	724.7	724.3
(H$_2$P^{4+} + 2HFBA$^-$ + H$_2$O)$^{2+}$/2	732.6	733.3
(H$_2$P^{4+} + 3HFBA$^-$ + H$^+$)$^{2+}$/2	831.6	831.3
(MnP^{5+} + HFBA$^-$)$^{4+}$/4	322.3	322.1
(MnP^{5+} + 2HFBA$^-$)$^{3+}$/3	501.0	500.5
(MnP^{5+} + 2HFBA$^-$ + H$_2$O)$^{3+}$/3	506.2	506.5
(MnP^{5+} + 3HFBA$^-$)$^{2+}$/2	857.6	857.2
(MnP^{5+} + 3HFBA$^-$ + H$_2$O)$^{2+}$/2	865.7	866.2

~1 μM solution of porphyrin and metalloporphyrin in 1:1 v/v acetonitrile:H$_2$O (containing 0.01% v/v heptafluorobutyric acid (HFBA)) mixture, 20 V cone voltage.

Table 3
Metal-centered reduction potential $E_{1/2}$ vs NHE (for $Mn^{III}P/Mn^{II}P$ redox couple), log k_{cat} for $O_2^{\cdot-}$ dismutation, and the lipophilicity of Mn porphyrin-based SOD mimics expressed in terms of partition between *n*-octanol and water, log P_{OW}.

Mn porphyrin	$E_{1/2}$/mV vs NHE[a]	log k_{cat}[b]	R_f	log P_{OW}[d]
MnTE-2-PyP^{5+}	+228	7.76 (cyt *c*) 7.73 (p.r.)[c]	0.055	-7.79
MnTnBu-2-PyP^{5+}	+254	7.25	0.209	-6.19
MnTnHex-2-PyP^{5+}	+314	7.48	0.355	-3.84
MnTnHep-2-PyP^{5+}	+342	7.65	0.427	-3.18
MnTnOct-2-PyP^{5+}	+367	7.71	0.500	-2.32
MnTMOE-2-PyP^{5+}	+251	8.04 (p.r.)[c]	0.082	-7.52
MnTMOHex-3-PyP^{5+}	+68	6.78	0.390	-5.45
MnTnBuOE-2-PyP^{5+}	+277	7.83	0.423	-4.10
SOD enzymes[e]	~ +300	8.84–9.30		

[a] $E_{1/2}$ is determined in 0.05 M phosphate buffer (pH 7.8, 0.1 M NaCl).
[b] k_{cat} was determined by cytochrome *c* assay in 0.05 M phosphate buffer (pH 7.8, at 25 ± 1 °C).
[c] p.r., pulse radiolysis.
[d] Data obtained from the relationship R_f vs log P_{OW} (log $P_{OW} = 12.207 \times R_f - 8.521$), and direct determinations of log P_{OW} for Mn(III) *N*-alkoxyalkylpyridylporphyrins [7].
[e] The data are taken from Refs. [28–30].

Consequently, the molecule is similarly lipophilic as MnTnHex-2-PyP^{5+} and *MnTnHep-2-PyP^{5+}* (Fig. 2). Moreover, as Mn ion approaches inner pyrrolic nitrogens, it makes transient bonds with oxygens, which greatly speeds up the metallation process. Transient bond formation, however, weakens the oxygen-butyl bond, and in turn an insignificant presence of the species with three butoxyethyl and one hydroxyethyl was found in a final preparation. With porphyrins that contain long alkyl chains, the steric hindrance prevented the easy approach of Mn ion to the porphyrin ring; the metallation of H_2TnHex-2-PyP^{5+} occurs at 100 °C, while within a few hours at room temperature in the case of MnTnBuOE-2-PyP^{5+}.

MnTnBuOE-2-PyP^{5+} and its metal-free ligand were characterized by thin-layer chromatography (R_f), elemental analysis, UV/vis spectroscopy, ESI-MS, and partition between *n*-octanol and water (log P_{OW}). The UV/vis data, the molar absorption coefficients, and the corresponding λ_{max} are given in Table 1, while the ESI-MS data are provided in Table 2.

The log $k_{cat}(O_2^{\cdot-})$, and the $E_{1/2}$ in mV vs NHE for $Mn^{III}P/Mn^{II}P$ redox couple are given in Table 3. As expected, the properties of MnTnBuOE-2-PyP^{5+} are dominated by the positive charges located on the pyridyl nitrogens, and by the presence of oxygen atoms in pyridyl substituents. When the pyridyl substituents are lipophilic, the cationic charges on nitrogens are not excessively solvated, and in turn exert a stronger electron-withdrawing effect on the Mn site: both MnTnHex-2-PyP^{5+} and MnTnHep-2-PyP^{5+} have ~100 mV more positive $E_{1/2}$ than MnTE-2-PyP^{5+}, indicating the less electron deficiency of the latter than of the former two porphyrins (Table 3). However, due to the presence of oxygens in alkyl chains, butoxyethyl chains are more solvated than hexyl or heptyl chains, which in turn hinders nitrogen charges (and thus suppresses their electron-withdrawing effect on the Mn site; consequently, the $E_{1/2}$ is less positive (Table 3). Additionally, the decrease in $E_{1/2}$ may occur as a consequence of the electron-donating properties of the alkoxyalkyl substituents. Further, the solvation of the porphyrin cavity formed by pyridyl substituents benefits the catalysis of $O_2^{\cdot-}$ dismutation as it involves the interaction of ionic species: singly charged Mn site and superoxide. Consequently, MnTnBuOE-2-PyP^{5+} is ~1.5- to 2-fold more potent catalyst of $O_2^{\cdot-}$ dismutation than its alkyl analogs, which has either the same number of carbon atoms in pyridyl substituents (MnTnHex-2-PyP^{5+}), or whose pyridyl substituents are of similar length (MnTnHep-2-PyP^{5+}) (Table 3).

The lipophilicity of Mn porphyrins has routinely and conveniently been measured by TLC retention factor, R_f. R_f is linearly related to the partition between *n*-octanol and water, log P_{OW} for the *ortho* and *meta* Mn(III) *N*-alkylpyridylporphyrins [15]. Herein we aimed to see if such relationship holds for the Mn(III) *N*-alkoxyalkylpyridylporphyrins also, and if therefore R_f could be used as a useful and convenient measure of their lipophilicity. Good agreement was found between the lipophilicity described by either R_f or log P_{OW} for both alkyl and alkoxyalkyl series of Mn porphyrins. Measured by log P_{OW} (but not R_f), and as expected due to the presence of oxygen atoms, MnTnBuOE-2-PyP^{5+} is slightly less lipophilic than MnTnHex-2-PyP^{5+} (Table 3).

S. cerevisiae study

Our earlier studies indicated that *E. coli* is overly sensitive to the lipophilic Mn porphyrins. They exert toxicity at >1 μM concentrations, which is in part due to their high cellular accumulation, micellar properties, and different redox activity of Mn site [11,12,31]. Thus, while efficacious at 1 μM, already at 5 μM MnTnHex-2-PyP^{5+} prevents *E. coli* growth. We have, however, observed that mammalian cells are less sensitive to lipophilic Mn porphyrins [32,33]. Our preliminary data indicated that eukaryotic yeast is also much less sensitive to the

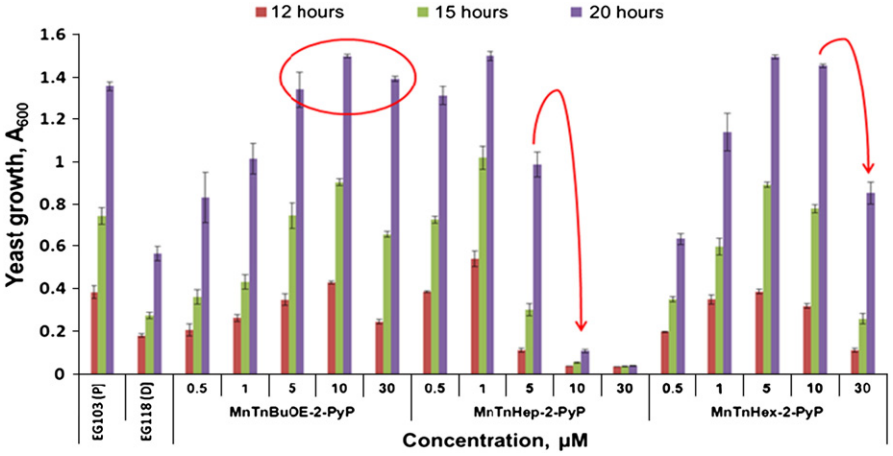

Fig. 3. Growth of the wild-type (EG 103) and SOD-deficient (*sod1*Δ) *S. cerevisiae* (EG118) in the presence and absence of lipophilic Mn porphyrins. The most efficacious is the most lipophilic compound, MnTnHep-2-PyP^{5+} (Table 3), presumably due to its highest accumulation in the cell, but is therefore also more toxic at ≥5 μM. MnTnHex-2-PyP^{5+} which is routinely toxic to SOD-deficient *E. coli* at >1 μM [11,31] is protective to SOD-deficient *S. cerevisiae* at up to 10 μM, and becomes toxic at 30 μM. MnTnBuOE-2-PyP^{5+} fully supports *S. cerevisiae* growth in the range of 5 to 30 μM.

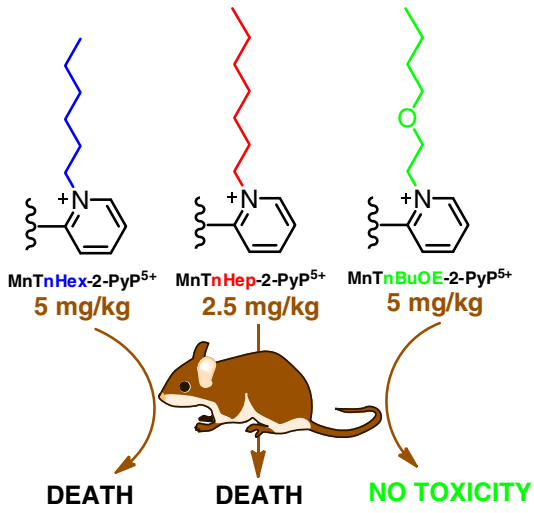

Fig. 4. Comparison of MnTnBuOE-2-PyP^{5+} to its alkyl analogs (MnTnHex-2-PyP^{5+} and MnTnHep-2-PyP^{5+}) with respect to the mice toxicity when given via single ip injection.

lipophilic Mn porphyrins and can tolerate well up to 30 μM MnTnHex-2-PyP^{5+} [34]. The aerobic growth of SOD-deficient *S. cerevisiae* (lacking Cu,ZnSOD) is thus a simple and excellent *in vivo* model of oxidative stress for evaluation of the therapeutic potential of lipophilic Mn porphyrins. MnTnBuOE-2-PyP^{5+} fully supports *S. cerevisiae* growth at 5–30 μM, and is of similar efficacy as MnTnHex-2-PyP^{5+}; however, at 30 μM MnTnHex-2-PyP^{5+} becomes toxic (Fig. 3). MnTnHep-2-PyP^{5+} is ~10-fold more lipophilic than MnTnHex-2-PyP^{5+} (Table 3). While of higher efficacy at only 0.5 and 1 μM than both MnTnHex-2-PyP^{5+} and MnTnBuOE-2-PyP^{5+}, MnTnHep-2-PyP^{5+} becomes toxic at ≥ 5 μM.

Mouse toxicity study

If injected ip at 2 mg/kg, MnTnHex-2-PyP^{5+} exerted transient toxicity; mice shivered and sat hunched for 60–90 min. The toxicity was more pronounced with 2.5 mg/kg; mice were barely walking and sometimes showed tail twist. One of four mice died, but the others recovered to some extent on the day after injection. All 4 mice died within a day after a single 5 mg/kg ip injection of MnTnHex-2-PyP^{5+}. However, all 4 mice injected with 5 mg/kg of MnTnBuOE-2-PyP^{5+} were briefly quiet immediately after injection, but were running in the cage the day afterward. Immediately on the single ip injection of 10 mg/kg of MnTnBuOE-2-PyP^{5+}, the mice looked sleepy and did not spontaneously ambulate; the next day they appeared better but not fully recovered. A tail twist and body shaking were seen with one mouse, but no mice died. Thus the toxicity of 10 mg/kg MnTnBuOE-2-PyP^{5+} appears similar or lower than that observed with 2.5 mg/kg of MnTnHex-2-PyP^{5+}. As expected, MnTnHep-2-PyP^{5+}—with pyridyl substituents of equal length, being a true analog of MnTnBuOE-2-PyP^{5+}—was much more toxic than MnTnHex-2-PyP^{5+}. All four mice which received single ip injections of 10 mg/kg MnTnHep-2-PyP^{5+}, 5 mg/kg MnTnHep-2-PyP^{5+}, or 2.5 mg/kg MnTnHep-2-PyP^{5+} died within 10–15 min, 20–45 min, and 24 h, respectively. Taken together, the data (shown in Fig. 4) indicate that MnTnBuOE-2-PyP^{5+} is at least 4-fold less toxic than MnTnHex-2-PyP^{5+} and MnTnHep-2-PyP^{5+}.

MnTnBuOE-2-PyP^{5+} was then injected ip twice daily for 7 days at doses up to 4.5 mg/kg (9 mg/kg total dose per day); no signs of toxicity were observed as measured by rotarod and body weight loss (Fig. 5). Even mice that underwent subarachnoid hemorrhage were fine with 2 daily injections of 4.5 mg/kg [Sheng et al., unpublished]—the single ip dose at which mice died if injected with hexyl or heptyl analogs. The total change in weight accounted for less than 5% when mice were injected twice daily with 4.5 mg/kg. With rotarod, improved performance was seen with almost all groups and at all times relative to the first day of injections; however, the changes did not reach statistical significance.

The lower toxicity of MnTnBuOE-2-PyP^{5+} relative to its hexyl and heptyl analogs is not fully understood at this point. The presence of oxygen atoms introduces the major differences among those compounds, and likely account to some extent for the substantial differences in their toxicity. Further experiments are under way to uncover possible relationships among the toxicity data, $E_{1/2}$ values for $Mn^{III}P/Mn^{II}P$ redox couple, solvation, charge distribution, and Mn-oxo chemistry of these water-soluble Mn porphyrin-based therapeutics.

Due to the excellent properties of MnTnBuOE-2-PyP^{5+}, we are intensifying efforts on its clinical development. The assessment of its plasma, tissue, and cellular and subcellular (mitochondrial and cytosolic) distribution is in progress, with the goal to understand the possible impact of the presence of oxygen atoms on the bioavailability of MnTnBuOE-2-PyP^{5+} when compared to the MnPs of similar lipophilicity, MnTnHex-2-PyP^{5+} and MnTnHep-2-PyP^{5+}.

Conclusions

While studying the mechanistic aspects involved in the preparation of the alkoxyalkyl series of Mn porphyrins (MnTMOHex-2(and 3)-PyP^{5+}), with the goal to reduce the toxicity of lipophilic *N*-alkylpyridylporphyrins, serendipity led us to the preparation of a new porphyrin molecule with a high therapeutic potential, MnTnBuOE-2-PyP^{5+}. The presence of the oxygen atoms and their positioning deeper within the hydrophobic long-alkyl chains make them less exposed to the solvent molecules, which in turn results in: (1) preserved lipophilicity of the molecule; (2) increased k_{cat} due to the more solvated cavity around the metal site; (3) disrupted micellar character which in turn resulted in a greatly diminished toxicity of MnTnBuOE-2-PyP^{5+} relative to its lipophilic alkyl analogs,

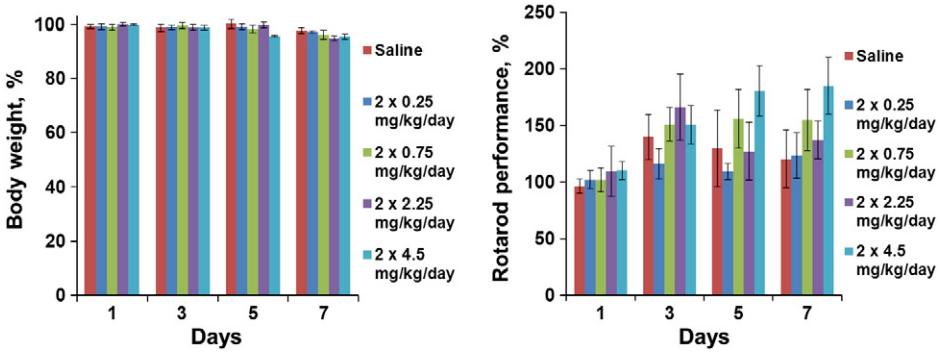

Fig. 5. Five groups of mice were treated with saline, 0.5, 1.5, 4.5, and 9 mg/kg/day ip total doses (given in two increments) for a week. Mice performance on rotarod and their weight were followed over a week. No significant toxicity of drug was measured by these two parameters.

MnTnHex-2-PyP^{5+} and MnTnHep-2-PyP^{5+} in both *S. cerevisiae* and mouse toxicity studies. In a very simple $O_2^{\cdot-}$ specific *in vivo* model, MnTnBuOE-2-PyP^{5+} proved efficacious in supporting aerobic growth of SOD-deficient *S. cerevisiae* to the extent of a wild yeast strain counterpart.

Acknowledgments

The authors acknowledge financial help from Duke University's CTSA Grant 1 UL 1 RR024128-01 from NCRR/NIH (A.T., I.B.H., I.S., M.L., H.S., D.S.W.), W.H. Coulter Translational Partners Grant Program (I.B.H., I.S., A.T.), and NIH/NCI Duke Comprehensive Cancer Center Core Grant (5-P30-CA14236-29) (I.S.), and IBH general research funds (Z.R.). I.B.H., I.S., and D.S.W. are consultants with BioMimetix Pharmaceuticals, Inc. L.B. acknowledges the financial support from Kuwait University, Grant MB01/09, and the excellent technical assistance of Milini Thomas.

References

[1] Batinic-Haberle, I.; Rajic, Z.; Tovmasyan, A.; Reboucas, J. S.; Ye, X.; Leong, K. W.; Dewhirst, M. W.; Vujaskovic, Z.; Benov, L.; Spasojevic, I. Diverse functions of cationic Mn(III) N-substituted pyridylporphyrins, recognized as SOD mimics. *Free Radic. Biol. Med.* **51:**1035–1053; 2011.

[2] Batinic-Haberle, I.; Reboucas, J. S.; Benov, L.; Spasojevic, I. Chemistry, biology and medical effects of water soluble metalloporphyrins. In: Kadish, K.M., Smith, K.M., Guillard, R. (Eds.), Handbook of porphyrin science. World Scientific, Singapore, pp. 291–393; 2011.

[3] Batinic-Haberle, I.; Reboucas, J. S.; Spasojevic, I. Superoxide dismutase mimics: chemistry, pharmacology, and therapeutic potential. *Antioxid. Redox Signal.* **13:** 877–918; 2010.

[4] Batinic-Haberle, I.; Spasojevic, I.; Stevens, R. D.; Hambright, P.; Neta, P.; Okado-Matsumoto, A.; Fridovich, I. New class of potent catalysts of O2.-dismutation. Mn(III) ortho-methoxyethylpyridyl- and di-ortho-methoxyethylimidazolylporphyrins. *Dalton Trans.*1696–1702; 2004.

[5] Batinic-Haberle, I.; Benov, L.; Spasojevic, I.; Fridovich, I. The ortho effect makes manganese(III) meso-tetrakis(*N*-methylpyridinium-2-yl)porphyrin a powerful and potentially useful superoxide dismutase mimic. *J. Biol. Chem.* **273:**24521–24528; 1998.

[6] Sheng, H.; Spasojevic, I.; Tse, H. M.; Jung, J. Y.; Hong, J.; Zhang, Z.; Piganelli, J. D.; Batinic-Haberle, I.; Warner, D. S. Neuroprotective efficacy from a lipophilic redox-modulating Mn(III) *N*-hexylpyridylporphyrin, MnTnHex-2-PyP: rodent models of ischemic stroke and subarachnoid hemorrhage. *J. Pharmacol. Exp. Ther.* **8:**906–916; 2011.

[7] Miriyala, S.; Spasojevic, I.; Tovmasyan, A.; Salvemini, D.; Vujaskovic, Z.; St. Clair, D.; Batinic-Haberle, I. Manganese superoxide dismutase, MnSOD and its mimics. *Biochim. Biophys. Acta.* **1822:**794–814; 2012.

[8] Batinic-Haberle, I.; Ndengele, M. M.; Cuzzocrea, S.; Reboucas, J. S.; Spasojevic, I.; Salvemini, D. Lipophilicity is a critical parameter that dominates the efficacy of metalloporphyrins in blocking the development of morphine antinociceptive tolerance through peroxynitrite-mediated pathways. *Free Radic. Biol. Med.* **46:** 212–219; 2009.

[9] Doyle, T.; Bryant, L.; Batinic-Haberle, I.; Little, J.; Cuzzocrea, S.; Masini, E.; Spasojevic, I.; Salvemini, D. Supraspinal inactivation of mitochondrial superoxide dismutase is a source of peroxynitrite in the development of morphine antinociceptive tolerance. *Neuroscience* **164:**702–710; 2009.

[10] Drobyshevsky, A.; Luo, K.; Derrick, M.; Yu, L.; Prasad, P.V.; Vasquez-Vivar, J.; Batinic-Haberle, I.; Tan, S. Oxidants in fetal brain reperfusion-reoxygenation injury trigger motor deficits. *J. Neurosci.* Under revision.

[11] Kos, I.; Benov, L.; Spasojevic, I.; Reboucas, J. S.; Batinic-Haberle, I. High lipophilicity of meta Mn(III) *N*-alkylpyridylporphyrin-based superoxide dismutase mimics compensates for their lower antioxidant potency and makes them as effective as ortho analogues in protecting superoxide dismutase-deficient *Escherichia coli*. *J. Med. Chem.* **52:**7868–7872; 2009.

[12] Okado-Matsumoto, A.; Batinic-Haberle, I.; Fridovich, I. Complementation of SOD-deficient *Escherichia coli* by manganese porphyrin mimics of superoxide dismutase activity. *Free Radic. Biol. Med.* **37:**401–410; 2004.

[13] Tovmasyan, A.; Rajic, Z.; Spasojevic, I.; Sheng, H.; Warner, D.; Li, A.; Gralla, E. B.; Benov, L.; Batinic-Haberle, I. Structural modification diminishes toxicity of lipophilic longer Mn(III) *N*-alkylpyridylporphyrin based powerful SOD mimics. Synthesis, characterization and SOD-deficient *E. coli* and *S. cerevisiae* studies. *Free Radic. Biol. Med.* **49:**S201; 2010.

[14] Reboucas, J. S.; Spasojevic, I.; Batinic-Haberle, I. Quality of potent Mn porphyrin-based SOD mimics and peroxynitrite scavengers for pre-clinical mechanistic/therapeutic purposes. *J. Pharm. Biomed. Anal.* **48:**1046–1049; 2008.

[15] Kos, I.; Reboucas, J. S.; DeFreitas-Silva, G.; Salvemini, D.; Vujaskovic, Z.; Dewhirst, M. W.; Spasojevic, I.; Batinic-Haberle, I. Lipophilicity of potent porphyrin-based antioxidants: comparison of ortho and meta isomers of Mn(III) *N*-alkylpyridylporphyrins. *Free Radic. Biol. Med.* **47:**72–78; 2009.

[16] Tipson, R. S. On esters of *p*-toluenesulfonic acid. *J. Org. Chem.* **9:**235–241; 1944.

[17] Batinić-Haberle, I.; Spasojević, I.; Stevens, R. D.; Hambright, P.; Fridovich, I. Manganese(III) *meso*-tetrakis(*ortho*-*N*-alkylpyridyl)porphyrins. Synthesis, characterization, and catalysis of $O_2^{\cdot-}$ dismutation. *J. Chem. Soc., Dalton Trans.*2689–2696; 2002.

[18] Lahaye, D.; Muthukumaran, K.; Hung, C. H.; Gryko, D.; Reboucas, J. S.; Spasojevic, I.; Batinic-Haberle, I.; Lindsey, J. S. Design and synthesis of manganese porphyrins with tailored lipophilicity: investigation of redox properties and superoxide dismutase activity. *Bioorg. Med. Chem.* **15:**7066–7086; 2007.

[19] Spasojevic, I.; Batinic-Haberle, I.; Stevens, R. D.; Hambright, P.; Thorpe, A. N.; Grodkowski, J.; Neta, P.; Fridovich, I. Manganese(III) biliverdin IX dimethyl ester: a powerful catalytic scavenger of superoxide employing the Mn(III)/Mn(IV) redox couple. *Inorg. Chem.* **40:**726–739; 2001.

[20] Eckshtain, M.; Zilbermann, I.; Mahammed, A.; Saltsman, A.; Okun, Z.; Maimon, E.; Cohen, H.; Meyerstein, D.; Gross, Z. Superoxide dismutase activity of corrole metal complexes. *Dalton Trans.*7879–7882; 2009.

[21] Lee, J.; Hunt, J. A.; Groves, J. T. Mechanisms of iron porphyrin reactions with peroxynitrite. *J. Am. Chem. Soc.* **120:**7493–7501; 1998.

[22] Lee, J.; Hunt, J. A.; Groves, J. T. Manganese porphyrins as redox-coupled peroxynitrite reductases. *J. Am. Chem. Soc.* **120:**6053–6061; 1998.

[23] Gralla, E. B.; Valentine, J. S. Null mutants of *Saccharomyces cerevisiae* Cu, Zn superoxide dismutase: characterization and spontaneous mutation rates. *J. Bacteriol.* **173:**5918–5920; 1991.

[24] Kaiser, C.; Michaelis, S.; Mitchell, A. Methods in yeast genetics. Cold Spring Harbor Laboratory Press, Cold Spring Harbor; 1994.

[25] Sheng, H.; Enghild, J. J.; Bowler, R.; Patel, M.; Batinic-Haberle, I.; Calvi, C. L.; Day, B. J.; Pearlstein, R. D.; Crapo, J. D.; Warner, D. S. Effects of metalloporphyrin catalytic antioxidants in experimental brain ischemia. *Free Radic. Biol. Med.* **33:** 947–961; 2002.

[26] Sheng, H.; Yang, W.; Fukuda, S.; Tse, H. M.; Paschen, W.; Johnson, K.; Batinic-Haberle, I.; Crapo, J. D.; Pearlstein, R. D.; Piganelli, J.; Warner, D. S. Long-term neuroprotection from a potent redox-modulating metalloporphyrin in the rat. *Free Rad. Biol. Med.* **47:**917–923; 2009.

[27] Reboucas, J. S.; Rajic, Z.; Tovmasyan, A.; Peixoto, I. N.; Spasojevic, I.; Benov, L.; Ventura, E.; do Monte, S. A.; Batinic-Haberle, I. Experimental and computational studies on Mn porphyrin-based therapeutics: unforeseen intramolecular rearrangements on methoxyalkyl analogues of MnTE-2-PyP^{5+} and MnTnHex-2-PyP^{5+}. *Free Radic. Biol. Med.* **51:**S148; 2011.

[28] Goldstein, S.; Fridovich, I.; Czapski, G. Kinetic properties of Cu, Zn-superoxide dismutase as a function of metal content–order restored. *Free Radic. Biol. Med.* **41:** 937–941; 2006.

[29] Vance, C. K.; Miller, A. F. A simple proposal that can explain the inactivity of metal-substituted superoxide dismutases. *J. Am. Chem. Soc.* **120:**461–467; 1998.

[30] Ellerby, R. M.; Cabelli, D. E.; Graden, J. A.; Valentine, J. S. Copper-zinc superoxide dismutase: why not pH-dependent? *J. Am. Chem. Soc.* **118:**6556–6561; 1996.

[31] Tovmasyan, A. G.; Rajic, Z.; Spasojevic, I.; Reboucas, J. S.; Chen, X.; Salvemini, D.; Sheng, H.; Warner, D. S.; Benov, L.; Batinic-Haberle, I. Methoxy-derivatization of alkyl chains increases the in vivo efficacy of cationic Mn porphyrins. Synthesis, characterization, SOD-like activity, and SOD-deficient E. coli study of meta Mn(III) *N*-methoxyalkylpyridylporphyrins. *Dalton Trans.* **40:** 4111–4121; 2011.

[32] Moeller, B. J.; Batinic-Haberle, I.; Spasojevic, I.; Rabbani, Z. N.; Anscher, M. S.; Vujaskovic, Z.; Dewhirst, M. W. A manganese porphyrin superoxide dismutase mimetic enhances tumor radioresponsiveness. *Int. J. Radiat. Oncol. Biol. Phys.* **63:** 545–552; 2005.

[33] Ye, X.; Fels, D.; Tovmasyan, A.; Aird, K. M.; de Deugd, C.; Allensworth, J. L.; Kos, I.; Park, W.; Spasojevic, I.; Devi, G. R.; Dewhirst, M. W.; Leong, K. W.; Batinic-Haberle, I. Cytotoxic effects of Mn(III) *N*-alkylpyridylporphyrins in the presence of cellular reductant, ascorbate. *Free. Radic. Res.* **45:**1289–1306; 2011.

[34] Spasojevic, I.; Li, A. M.; Tovmasyan, A.; Rajic, Z.; Salvemini, D.; St. Clair, D.; Valentine, J. S.; Vujaskovic, Z.; Gralla, E. B.; Batinic-Haberle, I. Accumulation of porphyrin-based SOD mimics in mitochondria is proportional to their lipophilicity. *Free Radic. Biol. Med.*S199; 2010.